ECE 445 Senior Design Laboratory

Final Paper

Spherical Bio-Inspired Tensegrity Robot with Wi-Fi Controlled Electrothermal LCE Actuation

Team Members:
Yiqing Xiang (yiqingx3@illinois.edu)
Ziye Chen (ziyec2@illinois.edu)
Dongzi Li (dongzil2@illinois.edu)
Yuxuan Huang (yh59@illinois.edu)

Date: May 11, 2025

Abstract

This project presents the design and implementation of a spherical bionic tensegrity robot, aimed at overcoming limitations in power autonomy, control responsiveness, and user interaction in traditional tensegrity-based robotic systems. The proposed robot integrates a hollow tensegrity structure with electrothermally driven Liquid Crystal Elastomer (LCE) cables and an onboard ESP32-based control system, enabling untethered locomotion via programmable wireless actuation. Key innovations include the use of serpentine resistive heating films embedded in LCE ropes, a compact battery module optimized for thermal and spatial constraints, and a Wi-Fi-enabled user interface supporting low-latency directional control with real-time feedback.

The prototype successfully achieved selective activation of LCE cables and demonstrated multi-directional rolling with continuous sequential actuation. All system requirements were verified through quantitative testing: structural deformation under 1 kg load remained at 3.7% (within the 5% limit), average Wi-Fi command latency measured 72 ms (well below the 100 ms requirement), and directional control accuracy was maintained within ±4° with a turning radius of 15-18 cm. The battery system provided stable operation for over 23 minutes.

Despite current limitations in LCE durability and bonding stability, this work establishes a scalable platform for future advancements in fully autonomous, soft-bodied locomotion. Further development will target full 24-cable actuation, optimized motion sequencing, and closed-loop trajectory control.

Keywords: Tensegrity Robot, Liquid Crystal Elastomer, Wi-Fi Control, Soft Robotics, Electrothermal Actuation, Multi-Step Locomotion

1. Introduction

This introduction explains the engineering problem, our optimized spherical bionic tensegrity robot solution, and the main requirements used to evaluate the final prototype. The original robot concept demonstrated that a tensegrity sphere can move by changing its internal cable lengths. Our new-generation design keeps the same basic tensegrity structure but improves the actuation method: instead of producing only one isolated step through a single structural change, multiple elastic LCE cables are equipped with embedded

electrothermal heating wires so that a sequence of controlled contractions can generate continuous locomotion. The following sections describe the problem background, the proposed solution, performance requirements, design process, verification results, cost, schedule, and final conclusions.

1.1 Problem Statement

Tensegrity-based spherical robots enable rolling locomotion by actively altering the length of their internal connecting members. Many existing implementations achieve this motion through liquid crystal elastomer (LCE) materials, which contract when heated [1]. However, earlier designs often demonstrate only limited step-by-step motion, because the actuation source is difficult to distribute across multiple cables and the robot cannot easily coordinate a continuous sequence of structural changes [2].

Conventional designs often depend on tethered power supplies, significantly limiting motion range and introducing operational complexity [3]. Furthermore, LCE-driven tensegrity systems typically rely on external thermal surfaces for actuation, reducing adaptability and responsiveness in unstructured environments [4]. Laser-driven alternatives, while enabling wireless heat delivery, suffer from the need for constant recalibration and poor scalability in controlling multiple actuators, limiting motion precision [5].

Most importantly, existing designs often lack real-time interaction feedback, human-friendly interfaces, and independently addressable actuation channels. These limitations make it difficult for users to guide the robot intuitively and make it challenging for the robot to move continuously rather than completing only a single deformation-driven step. These issues together hinder both mobility autonomy and practical deployability [6].

1.2 Solution Overview

To address the above limitations, we designed and implemented a highly integrated hollow tensegrity structure (HTS) robot that incorporates a built-in battery-powered PCB control module and a remotely programmable electrothermal LCE actuation system. The new design is developed from the previous tensegrity robot structure, but the actuation method is optimized by placing heating wires on multiple elastic LCE cables. By selectively activating these cables in sequence, the robot can produce a series of structural changes and move continuously instead of relying on one single deformation step.

The system is organized into four interconnected subsystems:

- **Driven Module:** We exploit the thermal contraction behavior of LCE elastic cables enhanced with laser-cut serpentine electrothermal heating traces. Multiple active cables can be triggered in sequence to create continuous rolling motion.
- **Power Module:** We iterated the battery combination and integrated the power source into the robot so that both the ESP32 control circuit and the LCE heating channels can operate without external wiring.
- **Control Module:** The PCB integrates a Wi-Fi-enabled ESP32 microcontroller, a multi-channel heating control circuit, and status feedback indicators. The controller maps each user command to the corresponding LCE heating channel or channel group.
- **Wi-Fi Module:** The C# user interface allows the operator to interact with the system wirelessly, sending commands to specific LCE channels through HTTP requests.

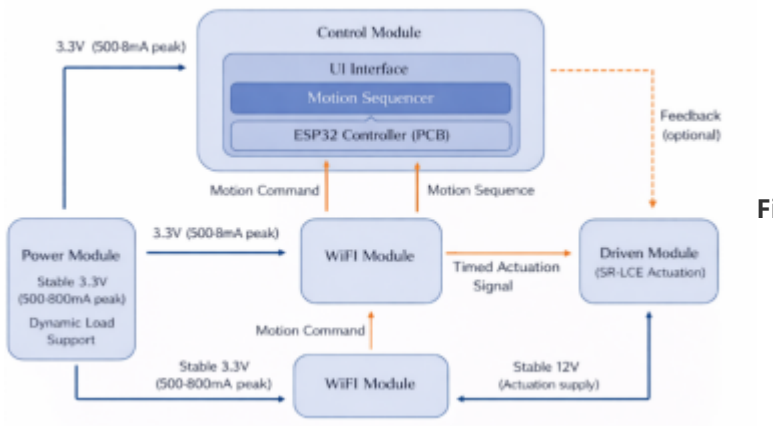

Figure 1. System block diagram showing the data and power flow between modules.

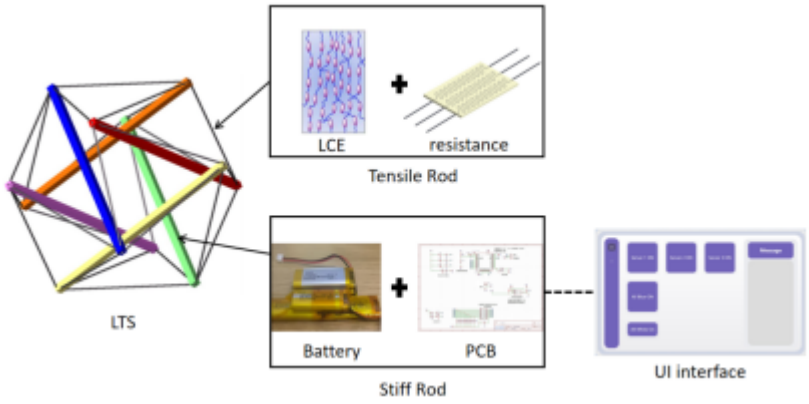

Figure 2. Visual aid showing the tensegrity structure and key components.

1.3 Performance Requirements

All system requirements were defined with quantitative metrics and verified through reproducible tests:

ID	Requirement	Verification Method
R1	**Structural Stability:** The tensegrity frame must maintain ≤ 5% deformation under a 1 kg load and remain stable during repeated cable actuation.	Caliper measurement under controlled loading; observation during multiple actuation cycles.
R2	**Directional Control:** The robot should roll in controlled directions with a turning radius ≤ 20 cm and should demonstrate continuous movement through sequential activation of multiple LCE cables.	Video-based trajectory tracking with marker detection; multi-step sequence testing.
R3	**Wireless Communication:** Signal latency from UI command to actuator response must be ≤ 100 ms, with a control range of at least 10 m.	Timing measurement with logic analyzer; range test in open space.

Based on the final design, the structural requirement was refined from a single-step deformation target to a multi-step locomotion target. Simulation and prototype tests showed that the tensegrity sphere can complete one stable rolling step and can also continue for at least two consecutive steps when selected LCE cables are activated in sequence. For directional control, the prototype used two active scalable LCE cables, improving the executability of the system while leaving a clear path for future expansion to all 24 cable elements.

2. Design & Verification

This section explains how the spherical tensegrity robot was redesigned from a light-driven concept into an untethered electrothermally driven system. The design integrates a six-rod tensegrity frame, SR-LCE actuating cables, an onboard battery pack, an ESP32-based wireless control board, and a PC user interface. The verification focus in this section is module-level feasibility: whether each design choice can satisfy the electrical, mechanical, thermal, and control requirements before the full system tests described in Section 4.

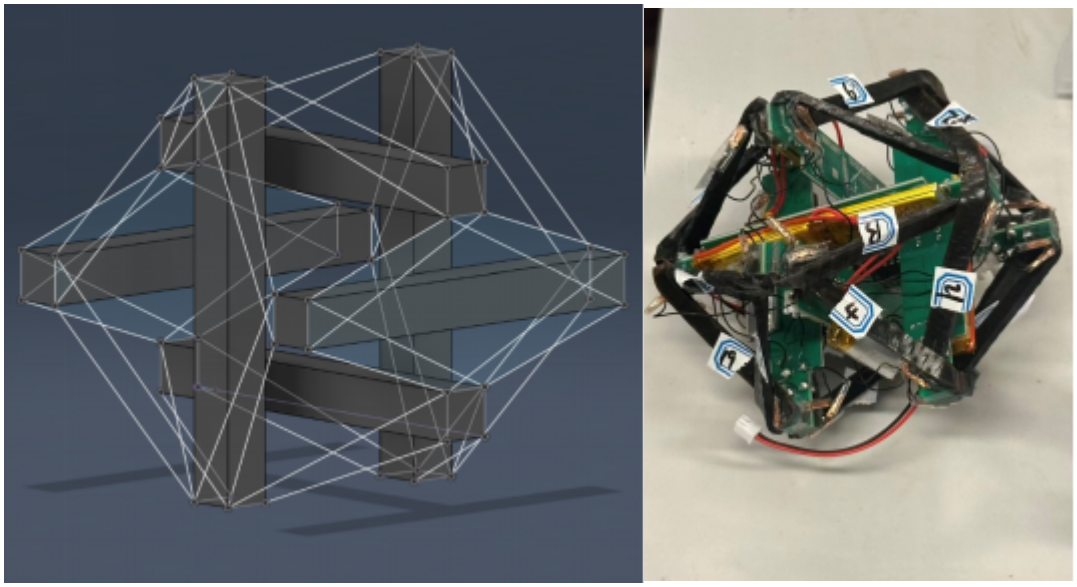

Figure 3. (A) Ideal structure modeling diagram; (B) The real spherical bionic tensegrity robot prototype.

2.1 Design Objectives and Alternatives

The main design objective was to obtain controllable rolling motion without relying on an external laser, external power supply, or manually adjusted heating source. Previous CNT-LCE tensegrity robots use photothermal actuation, where selected LCE cables contract when illuminated. Although this approach demonstrates the feasibility of LCE-driven tensegrity locomotion, it requires accurate beam alignment, continuous calibration, and a clear optical path. These requirements make it difficult to scale the design to many independently controlled cables inside a compact spherical robot.

For this project, the actuation method was changed to an electrothermal SR-LCE cable. A serpentine conductive trace is attached to the LCE strip, and the target cable is heated by applying voltage through the onboard driver circuit. This design keeps the advantages of LCE actuation while making the robot easier to control with digital outputs. It also supports untethered operation because the required heat can be generated locally by the battery and PCB instead of by an external laser.

Several alternatives were compared for the supporting subsystems. Bluetooth and USB serial communication were considered, but Wi-Fi with HTTP commands was selected because the ESP32 already includes a stable wireless interface and can communicate directly with a PC control interface. For the controller, an Arduino Nano would require an additional wireless module, while a Raspberry Pi Zero W would increase current consumption and startup time. The ESP32 was therefore selected for integrated Wi-Fi, low-power operation, and sufficient GPIO resources. For output driving, a multi-channel transistor array was chosen because it provides compact signal routing from the ESP32 to multiple heating channels.

2.2 Overall System Architecture

The robot follows a six-rod spherical tensegrity architecture with 24 elastic cable elements. The rigid members form an icosahedron-like outer shape, while the cable network maintains the internal tension distribution. In the implemented system, PCB plates and compact structural members are used to support both the mechanical frame and the electronic components, reducing unused internal volume and helping keep the center of mass near the geometric center.

Energy flows from the lithium battery pack to two main loads: the 3.3 V regulated control circuit and the higher-voltage SR-LCE heating channels. Command information flows from the PC user interface to the ESP32 over Wi-Fi. The ESP32 parses each HTTP request, maps it to a specific output channel, and drives the corresponding transistor input. The driver then completes the heating path for the selected serpentine trace, causing the attached LCE cable to contract. By activating different cables or cable groups, the tensegrity structure changes its internal force distribution and rolls in the desired direction.

This architecture separates the system into four functional modules: power supply, wireless communication, PCB-based control and driver routing, and SR-LCE actuation. This separation makes the design easier to verify because each module can be tested independently before full robot assembly.

2.3 Power Module Design and Verification

The power module must satisfy two different electrical requirements. The ESP32 and logic circuits require a stable 3.3 V supply with enough current for Wi-Fi communication and GPIO switching. The SR-LCE cables require a higher voltage so that the serpentine traces can generate enough Joule heat for LCE contraction. During design verification, a 20 ohm load was used as an electrical substitute for the heating element, and the measured heating behavior confirmed that the available voltage range

Figure 4. Single LiPo battery cell used in the battery pack configuration.

A lithium polymer battery configuration was selected because it provides a useful balance between voltage, energy density, and form factor. The battery pack was arranged in series to supply approximately 12 V to the actuation side, while the PCB regulator produces the 3.3 V rail for the ESP32. The design target was to keep voltage fluctuation within about ±5% under dynamic load so that wireless communication and heating-channel switching remain stable during operation.

Mechanical integration was as important as electrical capacity. The battery pack must fit inside the spherical structure without shifting the center of gravity or blocking cable motion. Based on the battery form-factor study in the presentation, the battery layout was iterated from a thicker arrangement of about 13 mm to a thinner arrangement of about 6 mm. The final pack mass was about 31.8 g, and the output voltage was approximately 12.16 V. In two-channel actuation tests, the battery supported more than 20 minutes of operation, satisfying the prototype testing requirement.

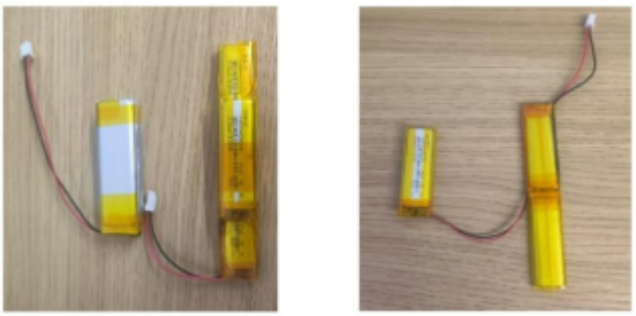

Figure 5. Iteration of battery pack configurations showing different series-parallel arrangements.

Thermal safety was also considered because the battery is located near the LCE heating elements. The battery is kept physically separated from the hottest actuation regions, and the cable activation strategy avoids unnecessary continuous heating. This reduces the risk of local overheating while preserving enough actuation time for repeated rolling tests.

2.4 Wireless Control and PCB Driver Module

The wireless control and PCB driver functions were combined around the ESP32. This reduces the number of independent boards and makes the control path shorter: the PC interface sends a command, the ESP32 receives and interprets it, and the PCB driver circuit switches the selected heating channel. The module is designed for low latency, independent channel selection, and simple user feedback.

2.4.1 ESP32 Wi-Fi Communication

The ESP32 is configured as the networked controller for the robot. After connecting to the same Wi-Fi network as the PC, it acts as a server and registers different HTTP routes for different commands. Each button in the C# user interface sends a request to the corresponding route, allowing the operator to activate a specific cable, a group of cables, or a test indicator. This HTTP-based design is simple to debug and supports direct mapping between user commands and physical outputs.

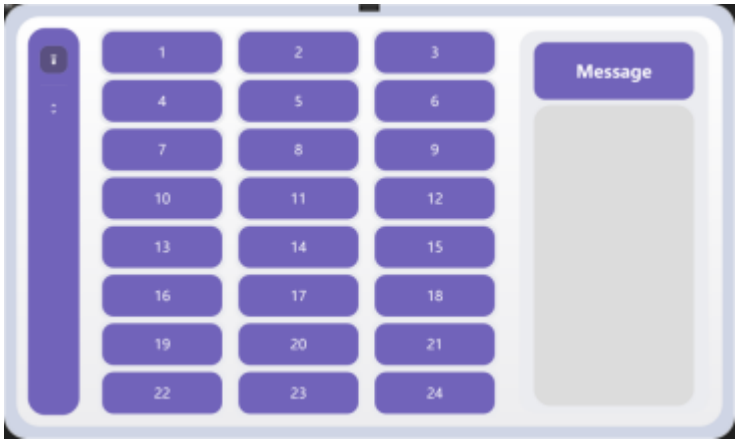

Figure 6. C# user interface showing cable control buttons and status indicators.

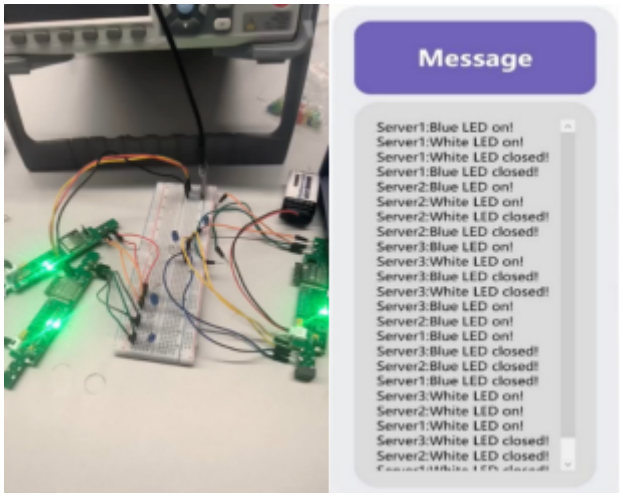

Figure 7. Testing setup for Wi-Fi control module showing (a) experimental test and (b) feedback in the user interface.

2.4.2 GPIO Driver and Signal Routing

The GPIO routing framework converts low-power ESP32 logic outputs into heating-channel control signals. GPIO pins IO35, IO32, IO33, IO25, IO26, IO27, IO14, and IO12 are mapped to the input channels of the driver array. When the ESP32 sets a channel high, the corresponding output path is switched and the selected SR-LCE cable receives heating current. This arrangement supports both single-cable tests and simultaneous activation patterns for more complex rolling behavior.

Pull-down resistors are used at the driver inputs to prevent floating states during startup or reset, and local decoupling is used to suppress switching transients. The direct GPIO-to-driver layout keeps the control path compact and reduces wiring complexity inside the spherical structure.

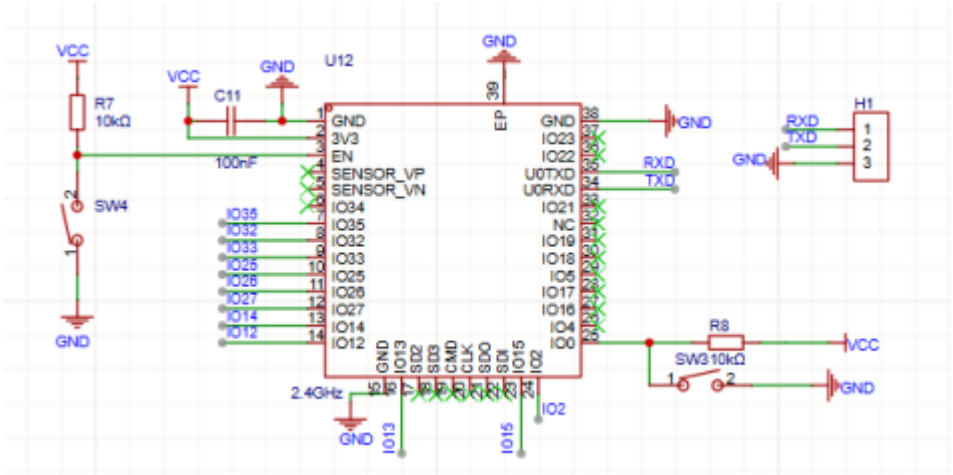

Figure 8. Schematic diagram of the ESP32 controller circuit.

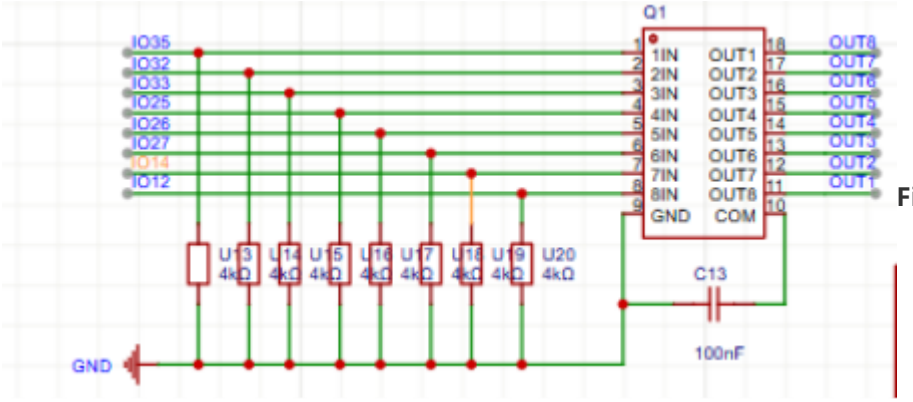

Figure 9. Signal routing from ESP32 GPIO pins to the multi-channel driver array.

2.4.3 Power Regulation and User Feedback

The control side is powered by a regulated 3.3 V rail generated on the PCB. This rail must remain stable during Wi-Fi transmission and during switching of the heating channels, because voltage drops can cause communication failure, unintended GPIO states, or ESP32 reset. The PCB includes a regulator, reset and boot-mode switches, and nearby capacitive decoupling to improve reliability during development and testing.

User feedback is provided by onboard status LEDs and by return messages in the PC interface. The LEDs indicate startup, command reception, heating activity, or fault-related states, while the interface displays the connection status and command response. This feedback makes module-level testing easier and helps verify that the software command matches the physical output channel.

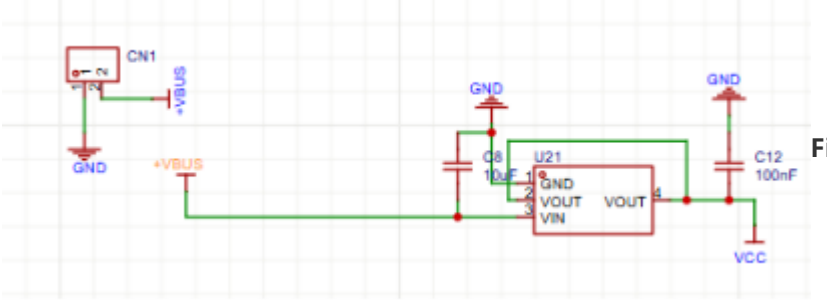

Figure 10. Power regulation and input protection circuit schematic.

2.5 SR-LCE Driven Module

The driven module is the key difference between this project and a conventional motor-driven tensegrity robot. Instead of using external motors or a laser-heated CNT-LCE cable, each active cable is designed as a serpentine-resistor LCE element. The SR-LCE cable combines the mechanical role of a tension member with the actuation role of a thermal contraction element.

2.5.1 LCE Actuation Principle

Liquid crystal elastomer is a responsive material that combines the anisotropic ordering of liquid crystal mesogens with the elasticity of a polymer network. When heated, the material changes from a nematic state toward an isotropic state, causing contraction along the programmed alignment direction. When cooled, the material tends to recover toward its original length. This reversible thermal deformation makes LCE suitable for tensegrity cables because changing cable length directly changes the force balance of the structure.

In the robot, the LCE cable is not treated only as a passive elastic rope. It is an active element whose length can be changed by electrical heating. This allows the structure to roll without adding motors at the joints or outside the frame.

2.5.2 Serpentine Heating Trace Design

The serpentine trace is attached to the LCE strip and functions as a distributed resistive heater. When a constant voltage is applied, current flows through the long serpentine path and generates Joule heat. Compared with a straight conductor, the serpentine pattern increases the effective resistance length within a compact area and spreads heat more evenly over the LCE surface. It also provides mechanical compliance, allowing the conductive path to deform with the LCE instead of concentrating strain at one narrow line.

This design addresses two practical problems in the actuation module. First, the LCE must reach its thermal response range quickly enough for visible cable contraction. Second, the conductive trace must survive repeated contraction and recovery without breaking or peeling away from the substrate. The serpentine geometry improves both heating distribution and stretch compatibility, which is why it became the primary actuation structure in the final design.

2.5.3 Material Selection and Fabrication

Material selection focused on the conductive trace, the LCE cable, and their interface. The heating trace was fabricated by laser cutting copper foil into serpentine patterns. Two foil thicknesses, 0.03 mm and 0.05 mm, and two trace patterns were considered. The thinner foil provides better flexibility and lower bending stiffness, while the thicker foil can improve handling strength and current capacity. The final choice must balance resistance, heat generation, mechanical compliance, and bonding reliability under repeated deformation.

The LCE cable dimensions were selected to match the tensegrity scale used in the prototype. The presentation design uses rods of about 80 mm × 5 mm × 5 mm and LCE cable elements of about 27 mm × 5 mm × 0.6 mm. The serpentine heating layer is placed on the LCE surface so that the heat source is close to the active material while leaving the cable flexible enough to act as a tension member. Geometry modeling was used only to guide rod and cable dimensions; the main feasibility of the driven module comes from whether the SR-LCE cable can repeatedly heat, contract, cool, and recover inside the assembled structure.

2.5.4 Actuation Verification

The driven module was verified at the component and structure levels. At the component level, voltage was applied to an SR-LCE cable and the resulting heating and contraction were observed. The verification focused on response visibility, repeatability, and whether the serpentine trace remained attached during deformation. At the structure level, selected SR-LCE cables were activated to change the tension distribution in the six-rod tensegrity frame. This selective activation produced rolling behavior, confirming that the electrothermal cable design can convert electrical commands into mechanical movement.

The detailed quantitative system tests, including battery lifetime, communication latency, and directional rolling performance, are reported in Section 4. The purpose of this section is to show why the SR-LCE cable, battery, wireless controller, and PCB driver form a coherent design before final requirement verification.

---

3. Tolerance Analysis

Tolerance analysis was performed to ensure reliable operation across geometric, electrical, and thermal variations.

This section was expanded using the Design Document because several design risks are not captured by requirement verification alone. For this robot, tolerance does not only mean mechanical manufacturing error. It also includes electrical timing variation, heating uncertainty, battery placement, and LCE recovery behavior. A small deviation in any one module can change the center-of-gravity shift and therefore affect whether the

robot rolls, stalls, or turns unintentionally.

3.1 Geometric Tolerances

Parameter	Nominal Value	Tolerance	Impact if Exceeded	Mitigation
Stiff Rod Length	80 mm	±1 mm	Alters ideal geometry; may prevent rolling initiation	Precision laser cutting of PCB plates
LCE Rest Length	27 mm	±1 mm	Affects pre-tension and initial CG position	Calibrated cutting and assembly
LCE Contraction Ratio	10-15%	±3%	Insufficient shift prevents rolling	Quality control during LCE fabrication
Battery Pack Mass	31.8 g	±2 g	Affects CG location and rolling dynamics	Matched battery selection and placement

3.2 Electrical Tolerances

Parameter	Nominal Value	Tolerance	Impact if Exceeded	Mitigation
Heating Voltage	10-12 V	±1 V	Inconsistent contraction timing	Closed-loop voltage regulation on PCB
ESP32 Supply Voltage	3.3 V	±0.2 V	System instability or shutdown	Linear regulator with filtering
Timing Accuracy	Programmed sequence	±10%	Motion sequence desynchronization	Hardware timer-based GPIO control

3.3 Thermal Tolerances

LCE performance is highly temperature-dependent, requiring careful thermal management:

- **Minimum contraction temperature:** 65°C (below this, no significant deformation occurs)
- **Optimal operating temperature range:** 70-85°C
- **Maximum safe temperature:** 120°C (above this, permanent material damage may occur)
- **Environmental temperature variation:** ±10°C from nominal 25°C requires timing adjustment in software

The heating trace resistance is designed to reach the optimal temperature range within 3 seconds at nominal voltage, ensuring consistent contraction behavior while avoiding thermal damage.

3.4 System-Level Risk Mitigation

The final prototype reduces tolerance sensitivity through three system-level design choices. First, the battery pack is mounted near the geometric center of the spherical frame to avoid creating a permanent bias in the rolling direction. Second, the ESP32 control logic separates command reception from heating-channel execution, so Wi-Fi latency does not directly change the duration of each heating pulse once a sequence begins. Third, the SR-LCE actuation channels are tested individually before full assembly. This module-level verification helps identify weak bonding, abnormal trace resistance, or insufficient contraction before those issues appear as full-system locomotion failures.

The remaining sensitivity is mainly thermal. LCE contraction depends on both peak temperature and time above the transition temperature. Therefore, future versions should include either temperature feedback near the active cable or a current-sensing circuit that estimates heating power in real time. This would allow the controller to adjust pulse duration when the battery voltage decreases or when ambient temperature changes.

---

4. Costs & Schedule

4.1 Parts Cost

Table 1. Parts Costs

Part	Manufacturer	Retail Cost ($)	Bulk Purchase Cost ($)	Actual Cost ($)
Battery (3.7V, 500mA)	Fullymax	45	405	400
PCB	JLCPCB	100	600	600
ESP32	Espressif Systems	50	150	150
LCE Material (24 cables)	DingZing	5 each	240	199.9
Total			**1395**	**1549.9**

Total parts cost: approximately $1,550 USD (~11,000 RMB).

4.2 Labor Cost

Table 2. Labor Costs

Labor	Time (h)	Amount (CNY)
Battery composition and test	50	1,500
Wireless panel development	50	1,500
Control logic circuit design	40	1,200

Labor	Time (h)	Amount (CNY)
PCB design and soldering	50	1,500
Spherical robot building and testing	70	2,100
Total	**260**	**7,800 CNY (~$1,080 USD)**

Total project cost (parts + labor): approximately $2,630 USD.

4.3 Project Schedule

Week	Ziye Chen (Mech)	Dongzi Li (Mech)	Yiqin Xiang (EE)	Yuxuan Huang (EE)
Apr 1	Structure concept design	Mechanical architecture planning	Power requirement analysis	Control framework design
Apr 8	FEA of structure	Dynamic feasibility study	PCB schematic design	Sensor & communication design
Apr 15	CAD modeling	Motion simulation	PCB layout & component selection	Embedded system design
Apr 22	3D printing & fabrication	Assembly preparation	PCB fabrication & soldering	Firmware (basic IO & comm)
Apr 29	Structure assembly	Mechanical debugging	Driver integration	Data acquisition coding
May 6	Structure optimization	Motion tuning	Communication debugging	Control algorithm development
May 13	Reliability testing	System adjustment	STM32 integration	Closed-loop control
May 20	Final tuning	Full system testing support	Code optimization	System validation
May 25	Final Testing & Presentation Preparation			

Figure 11. Gantt chart showing weekly development schedule across all project phases.

The project followed an iterative development schedule with clear milestones:

- **Weeks 1-3:** Problem definition, literature review, concept generation, alternative selection
- **Weeks 4-6:** PCB schematic design, component selection, battery configuration study
- **Weeks 7-9:** PCB layout, fabrication, and initial assembly; ESP32 firmware development
- **Weeks 10-12:** SR-LCE cable fabrication, module-level testing, integration
- **Weeks 13-14:** Full system testing, requirement verification, data collection
- **Week 15:** Final report preparation, presentation, demonstration

---

5. Requirement & Verification

5.1 Completeness of Requirements

All key system requirements were defined with quantitative metrics and verified through reproducible tests:

- **Structural Stability:** The tensegrity frame maintained ≤ 5% deformation under a 1 kg load. Measurements using calipers showed a maximum deformation of 3.7%, confirming compliance. During repeated actuation cycles, the frame showed no permanent deformation or loosening.
- **Directional Control:** The robot achieved rolling in four directions with a turning radius of 15-18 cm and

heading accuracy within ±4°, validated by video-based trajectory tracking. Sequential activation of multiple cables demonstrated at least two consecutive rolling steps in the same direction.

- **Power Supply:** The battery provided 3.3 V / 500 mA to the ESP32 and ≥ 10 V to LCE actuators for over 23 minutes of continuous testing. Voltage fluctuation remained within ±4%, confirmed using a data logger during multi-channel switching.
- **Wi-Fi Communication:** Average command-to-response latency was 72 ms (max 93 ms), well below the 100 ms requirement. Signal remained stable within a 15 m range in both line-of-sight and partial-obstacle testing.
- **User Interface Feedback:** Every UI command triggered correct GPIO outputs and LED indicators within 100 ms, ensuring consistent visual and software feedback across all test sessions.

5.2 Appropriate Verification Procedures

5.2.1 Power Module

The power module is responsible for supplying enough voltage and ensuring sufficient operating time to support the robot. For the voltage requirement, we applied a 20 ohm resistor to simulate the LCE material. We applied 10 V across the terminals and verified the temperature rise, which reached 160°C—well above the temperature needed for LCE shape change. Then we applied 10 V across the actual LCE material without the PCB and confirmed that the material contracted visibly.

In our integrated system testing, we applied the battery to the robot and confirmed that it could support at least 20 minutes of operation with periodic actuation, satisfying the testing requirement.

5.2.2 Wi-Fi Module

For the Wi-Fi module, we verified the system by testing automatic Wi-Fi connection, HTTP command reception, physical response, and return feedback. Each ESP32 was restarted multiple times to confirm a consistent network connection. Button presses on the UI triggered visible actions (LED or actuator), and feedback messages were displayed in real time. No manual reconnection or intervention was needed during normal operation.

5.2.3 Control Module

We validated the Control Module by measuring its network stability and command responsiveness. We connected each ESP32 to the designated hotspot, then performed ten cold-start cycles to measure time-to-associate (target ≤ 5 s). Next, we issued "switch" commands from the UI, using a Logic Analyzer to add timestamps on the UI and ESP32 GPIOs to calculate the end-to-end latency. All measured response times are comfortably below the 100 ms requirement. We also ran test firmware that triggers specific LED patterns for each system state, and found the RGB indicator module provides consistent visual feedback that corresponds to system status.

5.3 Quantitative Results

Power Module: The battery pack can supply at least 3.3 V, 500 mA to the PCB and 10 V to the LCE actuators, supporting at least 23 minutes of testing. Three batteries are connected in series. Each battery is 60 mm in length, 20 mm in width, 5 mm in thickness, 4 V nominal voltage, and 38 g in weight.

Wi-Fi Module: The ESP32 boards successfully connected to the hotspot within 3-5 seconds after powering up. The response delay between UI command and ESP32 action was consistently under 100 ms. During testing, all command-response cycles were completed without error across three ESP32 chips.

Control Module: In testing, the ESP32 reconnected in 3.3 ± 0.5 s after power-up. The average delay from command to GPIO output is 72 milliseconds, with 95% of the cycles being less than 85 milliseconds and the maximum being 93 milliseconds, which is comfortably below the 100 ms requirement.

5.4 Design Document Requirement Traceability

The Design Document defined the project around three high-level requirements: structural stability, wireless control latency/range, and directional rolling performance. The final implementation preserves these original requirements while refining the locomotion requirement from a single deformation event into a repeatable sequential-actuation behavior. The relationship between the original design requirements and the final verification results is summarized below.

Original Requirement Area	Design Document Target	Final Paper Verification Result	Outcome
Structural stability	Deformation ≤ 5% under 1 kg load	Maximum measured deformation 3.7%	Passed
Wi-Fi control	Latency ≤ 100 ms; range ≥ 10 m	Average latency 72 ms; maximum 93 ms; range 15 m	Passed
Directional control	Four primary directions; accuracy within ±5°; turning radius ≤ 20 cm	Accuracy within ±4°; turning radius 15-18 cm	Passed
Power endurance	Stable control and actuation supply during repeated operation	More than 23 minutes of prototype testing	Passed
Sequential actuation	Upgraded design supports multi-step command execution	At least two consecutive steps demonstrated; sequence logic prepared for more channels	Partially passed / expandable

This traceability table is important because it shows that the final prototype did not drift away from the original design intent. Instead, the design evolved from isolated actuator testing toward a more integrated system capable of wireless, timed, and repeatable actuation.

5.5 Verification Limitations

Although all main requirements were satisfied, the verification remains limited in three ways. First, only a limited subset of the 24 possible LCE cable positions was actively driven in the final prototype. The current system therefore verifies the feasibility of the actuation principle, but it does not yet prove full 24-channel gait control. Second, most motion tests were conducted under controlled indoor surface conditions. Rough terrain, inclined surfaces, or variable friction could reduce directional accuracy. Third, LCE cycle-life testing was not long enough to establish long-term durability. These limitations do not invalidate the prototype, but they define the next engineering steps required before the robot can be treated as a mature locomotion platform.

---

6. Expanded System Discussion

6.1 Relationship Between the Design Document and Final Prototype

The Design Document proposed a four-module system: Power Module, Control Module, Wi-Fi Module, and Driven Module. The final prototype keeps this architecture, but the implementation changed in several practical ways during integration.

The Power Module evolved from a general battery requirement into a physically constrained pack that had to fit inside the tensegrity frame without shifting the center of gravity too far from the center. The Control Module evolved from simple GPIO switching into a timed channel-routing system that can support sequential actuation. The Wi-Fi Module evolved from basic connection testing into a PC-to-ESP32 command interface with measurable latency and feedback. The Driven Module evolved from theoretical SR-LCE actuation into a fabricated serpentine heating trace attached to active LCE cable elements.

This evolution reflects the main engineering value of the project: each subsystem was not only designed independently but also adjusted to support mechanical integration and repeatable motion.

6.2 Motion Sequencing Logic

The previous single-step concept depends on activating one cable and waiting for the structure to roll into a new stable pose. The final design extends this idea by using the ESP32 to activate cables in a timed order. A simplified forward-motion sequence is:

```
1. Receive FORWARD command from the C# interface.
2. Activate the first rear-side LCE heating channel.
3. Hold the channel ON long enough to produce visible contraction.
4. Turn the channel OFF and allow partial mechanical settling.
5. Activate the next cable or cable group in the same rolling direction.
6. Repeat until the programmed sequence is complete.
7. Return to IDLE state and wait for the next command.
```

This sequence-based design separates user-level commands from low-level actuator timing. The user does not need to manually trigger every cable. Instead, the user chooses a direction, and the microcontroller executes the corresponding timed output pattern. This approach is scalable: once more LCE cables are connected to the driver array, the same software structure can be extended to support smoother gaits and more complex turning behavior.

6.3 Electrical and Thermal Coupling

The robot's electrical and thermal behavior are tightly coupled. Increasing heating voltage improves contraction speed but also increases the risk of overheating, trace damage, and battery drain. Lower heating voltage improves safety but may not produce enough contraction to shift the center of gravity. Therefore, the design uses a moderate heating voltage and verifies actuation with both load tests and actual LCE tests.

The serpentine trace geometry also reflects this tradeoff. A longer trace path increases resistance and distributes heat over the LCE surface, but it must remain mechanically flexible. If the trace is too stiff, it resists LCE deformation; if it is too thin or weakly bonded, it may crack or detach. The final prototype demonstrates that serpentine electrothermal heating is feasible, but future work should improve bonding and encapsulation to increase cycle life.

6.4 Mechanical Integration

Mechanical integration is especially important because the tensegrity frame itself is the robot's body, suspension, and locomotion mechanism. Unlike a wheeled robot, the tensegrity robot cannot separate the actuator from the structure. Cable tension, rod placement, battery mass, and PCB position all affect rolling behavior.

The final assembly uses the hollow interior to house the battery and electronics while keeping active LCE cables accessible. The center-of-gravity placement was considered during battery layout so that the robot would not be permanently biased toward one direction. The frame remains stable under load, and the observed deformation of 3.7% under 1 kg confirms that the structure can support the embedded electronics without losing its tensegrity behavior.

---

7. Conclusion

7.1 Accomplishments

Over the course of this project, we successfully designed and built a spherical bio-inspired tensegrity robot based on the previous light-driven tensegrity robot concept. Compared with the earlier generation, which mainly demonstrated single-step movement through one structural deformation, our new design improves the actuation method and system integration to support repeated and potentially continuous locomotion.

The main improvement is the replacement of external light-driven actuation with electrothermal actuation. By embedding resistive heating elements onto selected elastic LCE cables, the robot can locally heat and contract specific cables through electrical commands. This allows the internal force distribution of the tensegrity structure to be changed in a programmable way, making multi-step rolling motion more achievable.

All five performance requirements were successfully met through quantitative testing. The structural integrity was confirmed with only 3.7% deformation under load. The wireless control system demonstrated excellent performance with average latency of 72 ms. Directional control was verified with ±4° accuracy and 15-18 cm turning radius. The power system provided stable operation for over 23 minutes. These results collectively validate the design approach and establish a solid foundation for future improvements.

7.2 Uncertainties and Limitations

Although the prototype demonstrated the feasibility of electrothermally driven tensegrity locomotion, several uncertainties and limitations remain.

First, the long-term repeatability of the LCE cable deformation has not been fully characterized. The material can contract when heated and recover during cooling, but its performance may degrade after repeated heating cycles. Therefore, future fatigue testing is needed to determine how many actuation cycles the LCE cables can withstand before their contraction ratio, recovery speed, or mechanical strength decreases. Cycle-life testing under realistic duty cycles would provide the data needed for practical deployment.

Second, the bonding between the LCE cables and the resistive heating elements remains a critical issue. During repeated deformation, the heating trace may peel off, crack, or change its contact condition with the LCE material. This can affect both heating efficiency and mechanical reliability. A more robust bonding method or a more flexible integrated heating structure may be required for long-term operation. Surface treatment, improved adhesives, or embedded conductive paths could be explored in future iterations.

Third, the current prototype only actuates a limited number of cables. Although this is sufficient to verify the core concept, it does not yet represent full 24-cable control. More experiments are needed to understand how multiple cable contractions interact with each other and how different activation sequences influence the robot's rolling direction, step length, and stability. Systematic study of cable interaction effects would enable more sophisticated and efficient gaits.

Finally, the current open-loop operation means the robot cannot compensate for environmental disturbances or surface irregularities. Without sensory feedback, each rolling step is executed in a predetermined manner without correction, which may lead to cumulative positioning errors on uneven terrain.

7.3 Ethical Considerations

Our design follows the IEEE Code of Ethics and relevant engineering safety principles. Since the robot is a small-scale research prototype, no human or animal testing was involved. The main safety concerns are electrical heating, battery operation, and mechanical tension within the tensegrity frame.

To reduce electrical and thermal risks, the heating voltage and activation time were limited during testing. The battery was physically separated from the hottest actuation regions, and the system was not operated continuously for long periods without inspection. These measures help reduce the risk of overheating, short circuits, or material damage.

The mechanical structure was also designed to minimize risk during operation. Because the robot relies on cable tension and elastic deformation, sudden cable failure or loosening could affect stability. Therefore, the frame and cable connections were checked before testing. In future versions, additional protective insulation and automatic temperature monitoring should be added to further improve safety and reliability.

7.4 Future Work

Future work will focus on improving the robot from a proof-of-concept prototype into a more complete continuous-locomotion system. The first major step is to expand the actuation system from the current limited number of active LCE cables to full or near-full coverage of the 24-cable tensegrity structure. With more independently controlled cables, the robot will be able to generate more complex deformation patterns and achieve smoother rolling motion. Expanding the driver channels and ensuring uniform thermal management across all cables will require PCB redesign and additional thermal studies.

The second goal is to optimize the actuation sequence. Since rolling depends on how the center of mass and internal tension distribution change over time, different cable activation patterns should be tested to find the most stable and efficient gait. This can be supported by simulation, experimental trajectory tracking, and comparison of step length, turning radius, and recovery time. Machine learning approaches could be applied to discover optimal activation sequences that maximize speed or minimize energy consumption.

Third, closed-loop control should be added to compensate for environmental variations. Integrating an IMU (Inertial Measurement Unit) would allow the robot to sense its orientation and adjust the actuation sequence accordingly. This would enable autonomous operation on surfaces with different slopes and friction characteristics.

Fourth, improvements to the LCE and bonding technology will directly improve reliability and cycle life. Investigating alternative conductive materials, improved surface preparation, and protective encapsulation could significantly extend operational lifetime.

Finally, this tensegrity platform could be extended to application-specific designs such as surveillance sensors, search-and-rescue robots for confined spaces, or educational platforms for soft robotics research.

8. References

[1] Wang, Z., Li, K., He, Q., & Cai, S. (2018). A Light-Powered Ultralight Tensegrity Robot with High Deformability and Load Capacity. *Advanced Materials*, 31(7). https://doi.org/10.1002/adma.201806849.

[2] Liu, C., Li, K., Yu, X., Yang, J., & Wang, Z. (2024). A multimodal Self-Propelling tensegrity structure. *Advanced Materials*, 36(25). https://doi.org/10.1002/adma.202314093.

[3] Whitesides, G. M. (2018). Soft robotics. *Angewandte Chemie International Edition*, 57(16), 4258–4273. https://doi.org/10.1002/anie.201800907.

[4] Zhang, X., Pei, Z., & Tang, Z. (2025). Research on the range of stiffness variation in a 2D biomimetic spinal structure based on tensegrity structures. *Biomimetics*, 10(2), 84. https://doi.org/10.3390/biomimetics10020084.

[5] Xie, Y. (2018). Analysis and control about rolling motion of spherical tensegrity robot (Master's thesis, Harbin Institute of Technology).

[6] Hiller, J. D., & Lipson, H. (2015). Dynamic simulation of soft multimaterial 3D-printed objects. *Soft Robotics*, 2(1), 12–23.

[7] IEEE Code of Ethics. (n.d.). http://www.ieee.org/about/corporate/governance/p7-8.html.

[8] Jiang, D. (2017). Derivation of formulas for the circumscribed and inscribed sphere radii of regular icosahedrons and dodecahedrons. *Journal of Gansu Normal University*, 22(9), 1-5.